

Bit-rate dependent performance degradation of the long-haul RZ-DPSK system using block type dispersion map

Hidenori Taga

National Sun Yat-Sen University, No.70 Lien-Hai Road, Kaohsiung 80424 Taiwan R.O.C.
hidenoritaga@mail.nsysu.edu.tw
<http://www.nsysu.edu.tw/ver2008/>

Abstract: Bit-rate dependent performance degradation was observed in the long-haul RZ-DPSK system using the block type dispersion map. The performance was degraded near the system zero dispersion wavelength, and it showed a spectral performance hole near the zero dispersion wavelength. The existence of the hole did not depend on the spectral efficiency of the system, but it depended on the bit-rate. The hole existed for lower bit-rate up to 5Gbit/s, but disappeared more than about 15Gbit/s.

©2009 Optical Society of America

OCIS codes: (060.2330) Fiber optics communications; (060.4510) Optical communications.

References and links

1. T. Inoue, K. Ishida, T. Tokura, E. Shibano, H. Taga, K. Shimizu, K. Goto, and K. Motoshima, "150km repeater span transmission experiment over 9,000km," in *European Conference of Optical Communication (ECOC)*, Stockholm, Sweden, 2004, paper Th4.1.3.
2. J.-X. Cai, M. Nissov, W. Anderson, M. Vaa, C. R. Davidson, D. G. Foursa, L. Liu, Y. Cai, A. J. Lucero, W. W. Patterson, P. C. Corbett, A. N. Pilipetskii, and N. S. Bergano, "Long-haul 40 Gb/s RZ-DPSK transmission with long repeater spacing," in *Optical Fiber Communication Conference*, Technical Digest (CD) (Optical Society of America, 2006), paper OFD3, <http://www.opticsinfobase.org/abstract.cfm?URI=OFC-2006-OFD3>.
3. C. Rasmussen, T. Fjelde, J. Bennike, F. Liu, S. Dey, B. Mikkelsen, P. Mamyshev, and P. Serbe, P. v. d. Wagt, Y. Akasaka, D. Harris, D. Gapontsev, V. Ivshin, and P. Reeves-Hall, "DWDM 40G Transmission Over Trans-Pacific Distance (10 000 km) Using CSRZ-DPSK, Enhanced FEC, and All-Raman-Amplified 100-km UltraWave Fiber Spans," *J. Lightwave Technol.* **22**, 203–207 (2004), <http://www.opticsinfobase.org/JLT/abstract.cfm?URI=JLT-22-1-203>.
4. N. S. Bergano, "Wavelength division multiplexing in long-haul transoceanic transmission systems," *J. Lightwave Technol.* **23**(12), 4125–4139 (2005), <http://www.opticsinfobase.org/JLT/abstract.cfm?URI=JLT-23-12-41>.
5. G. Mohs, W. T. Anderson, and E. A. Golovchenko, "A New Dispersion Map for Undersea Optical Communication Systems," in *Optical Fiber Communication Conference and Exposition and The National Fiber Optic Engineers Conference*, OSA Technical Digest Series (CD) (Optical Society of America, 2007), paper JThA41, <http://www.opticsinfobase.org/abstract.cfm?URI=OFC-2007-JThA41>.
6. S. Dupont, and P. Marmier, L. d. Mouza, G. Charlet, and V. Letellier, "70 x 10 Gbps (mixed RZ-OOK and RZDPSK) upgrade of a 7224km conventional 32 x 10 Gbps designed system," in *European Conference of Optical Communication (ECOC)*, Berlin, Germany, 2007, Paper 2.3.5.
7. H. Taga, S.-S. Shu, J.-Y. Wu, and W.-T. Shih, "A theoretical study of the effect of the dispersion map upon a long-haul RZ-DPSK transmission system," *IEEE Photon. Technol. Lett.* **19**(24), 2060–2062 (2007), <http://ieeexplore.ieee.org/stamp/stamp.jsp?arnumber=4390960&isnumber=4390052>.
8. H. Taga, S.-S. Shu, J.-Y. Wu, and W.-T. Shih, "A theoretical study of the effect of zero-crossing points within the dispersion map upon a longhaul RZ-DPSK system," *Opt. Express* **16**(9), 6163–6169 (2008), <http://www.opticsinfobase.org/oe/abstract.cfm?URI=oe-16-9-6163>.
9. J.-X. Cai, C. R. Davidson, M. Nissov, H. Li, W. T. Anderson, Y. Cai, L. Liu, A. N. Pilipetskii, D. G. Foursa, W. W. Patterson, P. C. Corbett, A. J. Lucero, and N. S. Bergano, "Transmission of 40-Gb/s WDM Signals Over Transoceanic Distance Using Conventional NZ-DSF With Receiver Dispersion Slope Compensation," *J. Lightwave Technol.* **24**(1), 191–200 (2006), <http://www.opticsinfobase.org/JLT/abstract.cfm?URI=JLT-24-1-191>.
10. R.-J. Essiambre, and P. J. Winzer, "Fibre nonlinearities in electronically pre-distorted transmission," in *European Conference of Optical Communication (ECOC)*, Glasgow, United Kingdom, 2005, paper Tu3.2.2.
11. X. Wei, X. Liu, and C. Xu, "Numerical simulation of the SPM penalty in a 10-Gb/s RZ-DPSK system," *IEEE Photon. Technol. Lett.* **15**(11), 1636–1638 (2003), <http://ieeexplore.ieee.org/stamp/stamp.jsp?arnumber=1237613&isnumber=27767>.

12. H. Taga, "Observation of bit-rate dependent spectral performance hole for the long-haul RZ-DPSK system with block type dispersion map," in *14th OptoElectronics and Communications Conference (OECC 2009)*, Hong Kong, 2009, paper FQ5.
-

1. Introduction

Return-to-zero differential phase shift keying (RZ-DPSK) modulation format is effective to improve the transmission performance of the long-haul optical fiber communication system, and several experimental reports prove this [1–3]. Dispersion map is a popular technology for the long-haul optical fiber communication system, and so-called "block type" dispersion map is generally used for the conventional intensity modulation direct detection (IM-DD) based system [4]. For the block type dispersion map, a combination of positive and negative dispersion fiber composes one dispersion block, and an entire system is composed of several dispersion blocks. Even though the block type dispersion map is effective to improve the IM-DD based system performance, the performance of 10Gbit/s based long-haul RZ-DPSK system with the block type dispersion map shows a performance degradation near the system zero dispersion wavelength [5,6], and the major reason is attributed to the self phase modulation (SPM) through a theoretical study [7,8]. On the other hand, such performance degradation is not observed in 40Gbit/s based long-haul RZ-DPSK system with the block type dispersion map [9]. This fact implies that the performance degradation near the system zero dispersion wavelength might have a bit-rate dependency.

In this paper, the performance of the long-haul RZ-DPSK system with the block type dispersion map is studied theoretically as a function of the bit-rate. The results showed that there exists the bit-rate dependent performance degradation near the system zero dispersion wavelength. The degradation is independent to the spectral efficiency, but it disappears for higher bit-rate of more than about 15Gbit/s.

2. Simulation model

Figure 1 shows a schematic diagram of the simulation model. There were optical transmitters (TX) to generate the RZ-DPSK signals. The PSK signal was assumed to be generated by a Mach-Zehnder modulator (MZM), and the waveform applied for the two arms of the MZM was a raised cosine with the non return-to-zero (NRZ) format. The RZ waveform was applied after the PSK modulation, and the waveform was also raised cosine. The duty ratio of the pulse was 50%. The bit rate was varied between 5Gbit/s and 20Gbit/s, and the pattern was 2^9 De Bruijn sequence. The multiplexer (MUX) did not have any wavelength selective function, and the modulated pattern of each transmitter was randomized at the output of the MUX. Three different sets of the initial pattern at the output of the MUX were simulated in order to reduce the pattern dependent XPM impact [10], and the obtained results were averaged over these three sets.

The transmission line comprised fibers and EDFA repeaters. To compose the block type dispersion map, non-zero dispersion shifted fiber (NZDSF) and conventional single mode fiber (SMF) were used. Table 1 shows the parameters of these fibers. Eight NZDSF spans and one SMF span composed one block, and the SMF span was placed in the center of the block (i.e., fifth span). Each NZDSF span comprised NZDSF1 and NZDSF2, and the NZDSF1 had large effective area, while the NZDSF2 had reduced dispersion slope. The averaged zero dispersion wavelength of the transmission line was set to 1550nm. Figure 2 shows the dispersion map. This dispersion map was selected because it was commonly used for the long-haul undersea systems [4,5]. The total transmission distance was 6300km. The output power and the noise figure of the EDFA repeater were set to +11dBm and 4.5dB, respectively. The repeater span length was 100km. The wavelength dependent gain of the repeater was ignored in this simulation.

The optical demultiplexer (DEMUX) had the second order Gaussian shape. The bandwidth of the DEMUX depended on the channel separation, and it was set to a half of the channel separation. The cumulative chromatic dispersion for each channel was compensated at the receiving end, and the residual dispersion after dispersion equalization was set to

100ps/nm. For the signal demodulation, difference of the optical phase was directly calculated from the optical field, and the performance was evaluated by the Q-factor obtained from the rails of 0 phase and π phase [11].

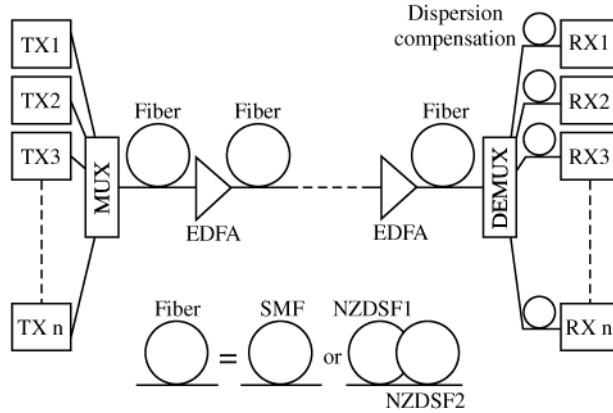


Fig. 1. A schematic diagram of the simulation model.

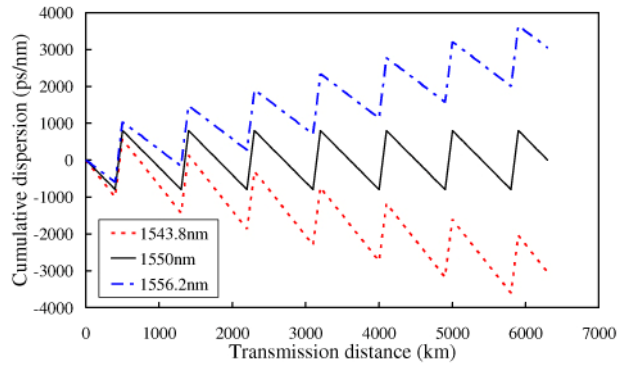


Fig. 2. Dispersion map of the simulated system

Table 1. Parameters of the transmission fiber

Parameter	NZDSF1	NZDSF2	SMF
Length (km)	50	50	100
Chromatic dispersion (ps/km/nm)	-2	-2	16
Dispersion slope (ps/km/nm ²)	0.1	0.06	0.06
Effective area (μm^2)	70	50	72
Loss (dB/km)	0.21	0.21	0.18
Nonlinear refractive index		2.6×10^{-20}	

3. Results and discussion

Two different conditions were simulated. The first one was the same spectral efficiency [12]. For this case, the spectral efficiency of the system was kept constant to 20%, and the number of channels was adjusted to keep the same total capacity of 320Gbit/s. The second one was the same wavelength allocation. For this case, the number of channels was set to 32, and the system capacity was varied from 160Gbit/s to 640Gbit/s.

3.1 Same spectral efficiency

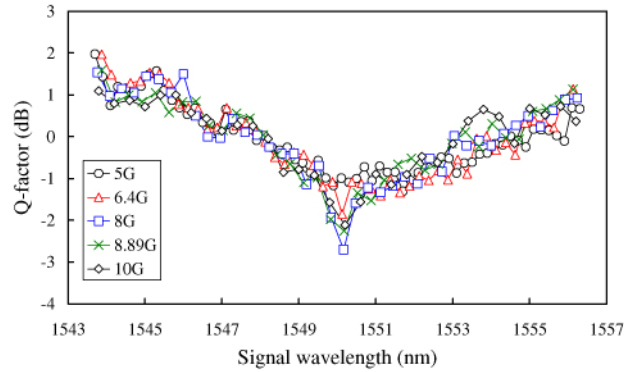
To maintain the same spectral efficiency for any bit-rate, number of wavelengths was varied as the bit-rate was varied, while the signal bandwidth was almost identical. Table 2 summarizes the allocations of the bit-rate, number of wavelength, signal wavelength band, and wavelength separation.

Table 2. Summary of simulated bit-rate and wavelengths

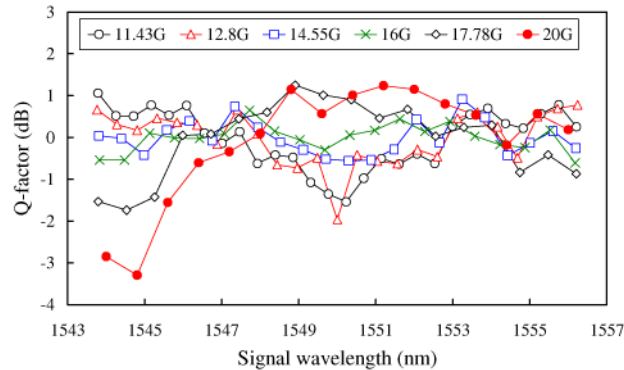
Bit-rate	Number of wavelength	Signal wavelength band	Wavelength separation
5G	64	1543.7 ~ 1556.3 nm	0.2nm
6.4G	50	1543.875 ~ 1556.125 nm	0.25nm
8G	40	1543.76 ~ 1556.24 nm	0.32nm
8.89G	36	1543.875 ~ 1556.125 nm	0.35nm
10G	32	1543.8 ~ 1556.2 nm	0.4nm
11.43G	28	1543.79 ~ 1556.21 nm	0.46nm
12.8G	25	1543.76 ~ 1556.24 nm	0.52nm
14.55G	22	1543.805 ~ 1556.195 nm	0.59nm
16G	20	1543.825 ~ 1556.175 nm	0.65nm
17.78G	18	1543.795 ~ 1556.205 nm	0.73nm
20G	16	1544.0 ~ 1556.0 nm	0.8nm

Figure 3 shows the relative Q-factor as a function of the signal wavelength and the bit-rate. The reference (i.e., 0dB in the Fig.) is set to the averaged value of the Q-factor for each bit-rate. Figure 3(a) shows the performance of less than 10Gbit/s, and Fig. 3(b) shows the performance of above 10Gbit/s. As seen in Fig. 3 (a), the spectral performance hole near the system zero dispersion wavelength was quite evident for any bit-rate. The width of the spectral hole was almost independent to the bit-rate. On the other hand, the spectral performance hole became smaller by increasing the bit-rate as shown in Fig. 3(b), and it disappeared around 15Gbit/s.

As shown in Fig. 3(b), the performances of shorter wavelength channels at 20Gbit/s showed notable degradations. The reason could be attributed to the same as the conventional IM-DD system. For the conventional IM-DD system, large cumulative dispersion combined with the fiber nonlinear effects causes the performance degradation of the edge channels of the WDM system [6]. For 20Gbit/s case, as the tendency of the performance is the same as the IM-DD case (i.e., the channels close to the zero dispersion wavelength show better performance while the edge channels show worse performance), it should be reasonable to consider that the reason is common for both cases.



(a) below 10Gbit/s



(b) above 10Gbit/s

Fig. 3. Relative Q-factor as a function of the bit-rate.

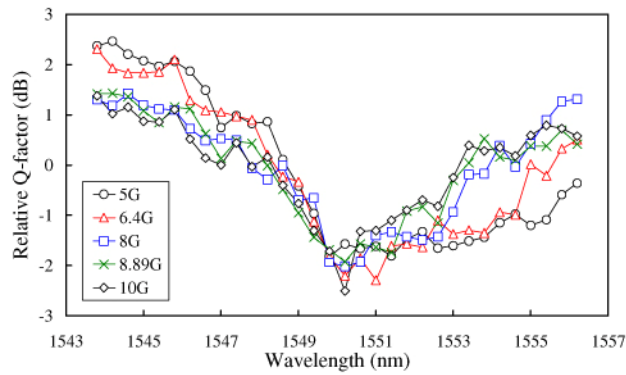
3.2 Same wavelength allocation

For the same spectral efficiency, the wavelength allocation was varied for different bit-rate. Then, the same wavelength allocation was investigated for comparison. Number of channels was 32, and the channel separation was 0.4nm. The signal wavelength ranged from 1543.8nm to 1556.2nm.

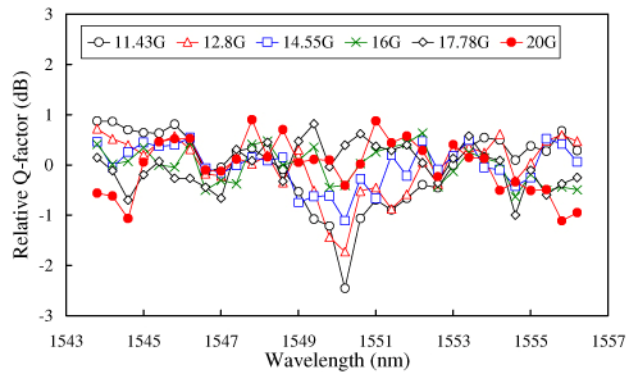
Figure 4 shows the relative Q-factor as a function of the signal wavelength and the bit-rate. The reference (i.e., 0dB in the Fig.) is set to the averaged value of the Q-factor for each bit-rate. Figure 4(a) shows the performance of less than 10Gbit/s, and Fig. 4(b) shows the performance of above 10Gbit/s. As seen in Fig. 4, the tendency was the same as Fig. 3.

From these results, it is obvious that there exists the spectral performance hole near the system zero dispersion wavelength, and it has the bit-rate dependence. Even though, there are a few notable differences in Figs. 3 and 4. Comparing Figs. 3(a) and 4(a), it is obvious that the performances of lower bit-rate and longer wavelength channels are degraded when the same channel allocation was adopted. The reason could be attributed to the channel power difference. For example, per channel power is twice for 5Gbit/s case when the same channel allocation was adopted. The increase of the channel power could be considered to cause the increase of the nonlinear impairment for the lower bit-rate.

Comparing Figs. 3(b) and 4(b), it is obvious that the performance of higher bit-rate becomes flatter for the same channel allocation. The reason could be attributed to smaller channel power for the same channel allocation. As a matter of fact, per channel power is a half for 20Gbit/s case for the same channel allocation. The decrease of the channel power could be considered to reduce the nonlinear impairment for the higher bit-rate.



(a) below 10Gbit/s



(b) above 10Gbit/s

Fig. 4. Relative Q-factor as a function of the bit-rate.

4. Conclusions

The bit-rate dependence in the long-haul RZ-DPSK system with the block type dispersion map was investigated. The spectral performance hole near the system zero dispersion wavelength was clearly observed for the lower bit-rate of less than around 15Gbit/s while the higher bit-rate did not exhibit the performance hole. Also, the existence of the performance hole did not depend on the spectral efficiency. As the fundamental physical mechanism of the performance hole is not clear, further studies are required to explain more details of this phenomenon.

Acknowledgments

This work is supported partially by National Science Council 96-2221-E-110-049-MY3, partially by key module technologies for ultra-broad bandwidth optical fiber communication project of Ministry of Economy, Taiwan, R.O.C., and partially by Aim for the Top University Plan of the National Sun Yat-Sen University and Ministry of Education, Taiwan, R.O.C.